Editors' Suggestion | Featured in Physics

Characterization and Control of the Run-and-Tumble Dynamics of *Escherichia Coli*

Christina Kurzthaler,[1,2,3,4,*] Yongfeng Zhao,[5,6,7,8,†] Nan Zhou,[9] Jana Schwarz-Linek,[10] Clemence Devailly,[10] Jochen Arlt,[10] Jian-Dong Huang,[6,11] Wilson C. K. Poon,[10] Thomas Franosch,[4] Julien Tailleur,[7,‡] and Vincent A. Martinez[10,§]

[1]*Max Planck Institute for the Physics of Complex Systems, 01187 Dresden, Germany*
[2]*Center for Systems Biology Dresden, 01307 Dresden, Germany*
[3]*Department of Mechanical and Aerospace Engineering, Princeton University, Princeton, New Jersey 08544, USA*
[4]*Institut für Theoretische Physik, Universität Innsbruck, Technikerstraße 21A, A-6020 Innsbruck, Austria*
[5]*Center for Soft Condensed Matter Physics and Interdisciplinary Research and School of Physical Science and Technology, Soochow University, Suzhou 215006, China*
[6]*School of Biomedical Sciences, Li Ka Shing Faculty of Medicine, University of Hong Kong, Pok Fu Lam, Hong Kong, China*
[7]*Université de Paris, MSC, UMR 7057 CNRS, 75205 Paris, France*
[8]*School of Physics and Astronomy and Institute of Natural Sciences, Shanghai Jiao Tong University, Shanghai 200240, China*
[9]*ZJU-Hangzhou Global Scientific and Technological Innovation Center, Zhejiang University, Hangzhou 311200, China*
[10]*School of Physics and Astronomy, University of Edinburgh, James Clerk Maxwell Building, Peter Guthrie Tait Road, Edinburgh EH9 3FD, United Kingdom*
[11]*CAS Key Laboratory of Quantitative Engineering Biology, Shenzhen Institute of Synthetic Biology, Shenzhen Institutes of Advanced Technology, Chinese Academy of Sciences, Shenzhen 518055, China*

(Received 21 December 2022; revised 29 November 2023; accepted 1 December 2023; published 19 January 2024)

We characterize the full spatiotemporal gait of populations of swimming *Escherichia coli* using renewal processes to analyze the measurements of intermediate scattering functions. This allows us to demonstrate quantitatively how the persistence length of an engineered strain can be controlled by a chemical inducer and to report a controlled transition from perpetual tumbling to smooth swimming. For wild-type *E. coli*, we measure simultaneously the microscopic motility parameters and the large-scale effective diffusivity, hence quantitatively bridging for the first time small-scale directed swimming and macroscopic diffusion.

DOI: 10.1103/PhysRevLett.132.038302

Swimming is key for many microorganisms to survive [1–8]. Such "active matter" is necessarily far from thermal equilibrium [9–12] and displays peculiar transport properties, which enable foraging [13] and escaping from harm [14]. The flagellated bacterium *Escherichia coli* is a model system for active matter experiments [3,15–21]. Much is known about its genetics, biochemistry, and ultrastructure, but relating this knowledge to the emerging phenotype, for instance to predict the three-dimensional (3D) pattern of locomotion (or gait) of a swimming population, remains a challenge.

The bacterium's "run-and-tumble" (RT) dynamics [2] alternates between persistent motion along the cell's axis and sudden changes of direction. While the motion of isolated flagella has been studied in detail using *in vitro* single-motor experiments [22,23], a quantitative characterization of the full 3D gait of swimming populations of multiflagellated bacteria has been out of reach so far. This stems, in particular, from the need for measurements over length scales ranging from the order of the short-time runs ($\sim$1–10 μm) to far beyond the persistence length ($\gtrsim 10^2$ μm). Assuming exponentially distributed run and tumble durations, the RT dynamics is predicted to lead to a large-scale diffusion [2,24–26], but this claim has seldom been demonstrated experimentally, and the underlying assumptions have recently been questioned [22,27]. The accurate characterization of RT dynamics will therefore fill an important gap.

At the same time, while many aspects of the motility of *E. coli* have been brought under direct experimental control [2,4,18,28–35], including the ability to regulate its run speed by light [36,37], there is currently only limited scope to fine-tune its overall gait compared to synthetic swimmers [38–43] because the bacterium's tumble dynamics is difficult to control independently. The aforementioned lack of good methods to quantify its RT dynamics contributes to these difficulties, which in turn limits the use of *E. coli* as a model organism for fundamental active matter research.

In this Letter, we report a full characterization of the 3D gait of *E. coli*, which enables us to demonstrate how the RT

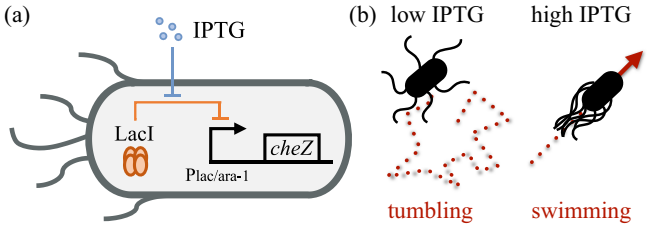

FIG. 1. Engineered strain NZ1. (a) Scheme of the regulation: *cheZ* expression driven by Plac/ara-1 is suppressed by the LacI suppressor. Exogenously adding IPTG induces *cheZ* expression by reducing LacI suppression. (b) Cells are expected to tumble continuously at low IPTG concentration and to enter a smooth swimming state at high IPTG concentration.

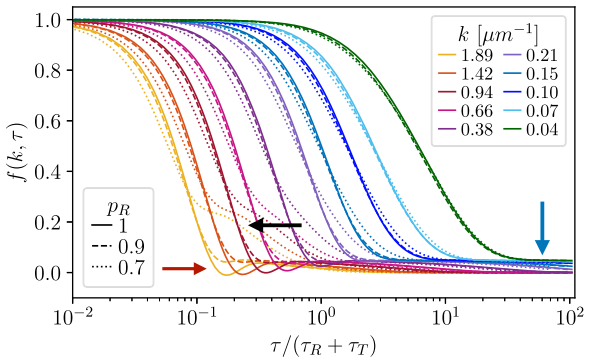

FIG. 2. Theoretical ISFs for a suspension comprising a fraction α of RT bacteria and $1-\alpha$ of diffusing cells, for several wave numbers k. We consider different fractions of run time $p_R = \tau_R/(\tau_R+\tau_T)$, using $\tau_R = 1$ s and $\tau_T = 0, 0.1, 0.5$ s, with $\bar{v} = 15\,\mu\mathrm{m\,s^{-1}}$, $\sigma_v = 4.5\,\mu\mathrm{m\,s^{-1}}$, $D = 0.3\,\mu\mathrm{m^2\,s^{-1}}$, and $\alpha = 0.95$. For smooth swimmers with fixed speed v_0, $f(k,\tau) = \mathrm{sinc}(v_0 k\tau)\exp(-Dk^2\tau)$. When $p_R = 1$, this leads to clear oscillations of $f(k,\tau)$ at small length scales (red arrow). As the tumbling rate τ_T^{-1} increases (black arrow), these oscillations are smeared out and the diffusive dynamics of the tumbling bacteria eventually leads to a diffusive plateau around $f \sim 1 - p_R$. At large but finite times, depending on the value of k, the diffusive cells may not have decorrelated, leading to a nonzero plateau of $f(k,\tau)$ (blue arrow).

dynamics of an engineered strain can be tuned from perpetual tumbling to smooth swimming as the concentration of a chemical inducer is varied. These cells can be used in future work under conditions in which their persistence length can be predicted *a priori* once experimental conditions are specified.

We characterize a bacterium's displacement $\Delta\mathbf{r}(\tau)$ at lag time τ in Fourier space using the intermediate scattering function (ISF):

$$f(\mathbf{k},\tau) = \left\langle e^{-i\mathbf{k}\cdot\Delta\mathbf{r}(\tau)} \right\rangle. \tag{1}$$

Analyzing the ISF with a renewal theory then allows us to extract microscopic kinetic parameters such as the particle speed and the run and tumble durations. To measure the ISF, we extend conventional differential dynamic microscopy (DDM) [44] to collect data encompassing both short-length-scale directed-swimming and large-length-scale diffusive regimes. DDM allows us to work in bulk fluid to minimize hydrodynamic interactions with surfaces [45–49]. It also circumvents the need of single-cell tracking, which requires customized Lagrangian [1,2,50,51] or holographic [52,53] microscopy and is limited by the need for low cell concentration, statistical accuracy, and short trajectories. Our data confirm to order of magnitude previous measurements of *E. coli* motility [1], albeit with a significantly larger run time. We find large-length-scale diffusive behavior and compare the extracted diffusivity, D_{eff}, with a theoretical prediction based on the microscopic motility parameters. The predicted D_{eff} is robust against experimental complexities, but speed fluctuations contribute ~10% of its value. Below, we focus on the biophysical implications of our results while our methodology is detailed and validated in a companion paper [54].

Bacterial strain.—We engineered the NZ1 strain by deleting the *cheZ* gene in *E. coli* K12 and adding the inducible plasmid Plac/ara-1-cheZ [17] [Fig. 1(a)]. Deleting *cheZ* suppresses the transition from clockwise to counterclockwise flagella rotation, so that cells tumble permanently. The plasmid restores expression of *cheZ* at a rate dependant on the concentration of Isopropyl β-d-1-thiogalactopyranoside (IPTG). It is expected, though never yet confirmed, that tuning the concentration of IPTG during the growth of this strain allows the control of RT dynamics [Fig. 1(b)]. Bacteria were cultured and resuspended carefully in motility buffer [3] to ensure a very high final motile fraction, $\alpha \gtrsim 95\%$ [55].

ISF measurement and analysis.—To characterize the gait of the NZ1 strain at different IPTG concentrations, we first measured its ISF by DDM. We then fitted it to the calculated ISF of a well-established model of RT bacteria [1,25,60–62] that is modified to account for recently observed intrinsic fluctuations of the propulsion speed [63]. In this model, bacteria run in quasistraight lines at speed v until they enter a tumbling phase, at rate τ_R^{-1}, during which they fully randomize their orientations. They resume swimming at rate τ_T^{-1} with a new swim speed, sampled from a Schulz distribution $p(v)$ characterized by a mean velocity $\bar{v}$ and a standard deviation σ_v [44]. (For an alternative way to account for swimming-speed fluctuations, see Ref. [54].) In addition, cells diffuse translationally with diffusivity D during both run and tumble phases. There is also a fraction $1-\alpha$ of nonmotile cells that undergo Brownian motion only, also with diffusivity D [64]. The ISF for a noninteracting *E. coli* suspension predicted by this model reads

$$f(k,\tau) = \alpha f_{\mathrm{RT}}(k,\tau) + (1-\alpha)e^{-Dk^2\tau}, \tag{2}$$

where $f_{\mathrm{RT}}(k,\tau)$ is the ISF of RT bacteria [54]. Measuring this ISF for a wide range of k and τ values then allows

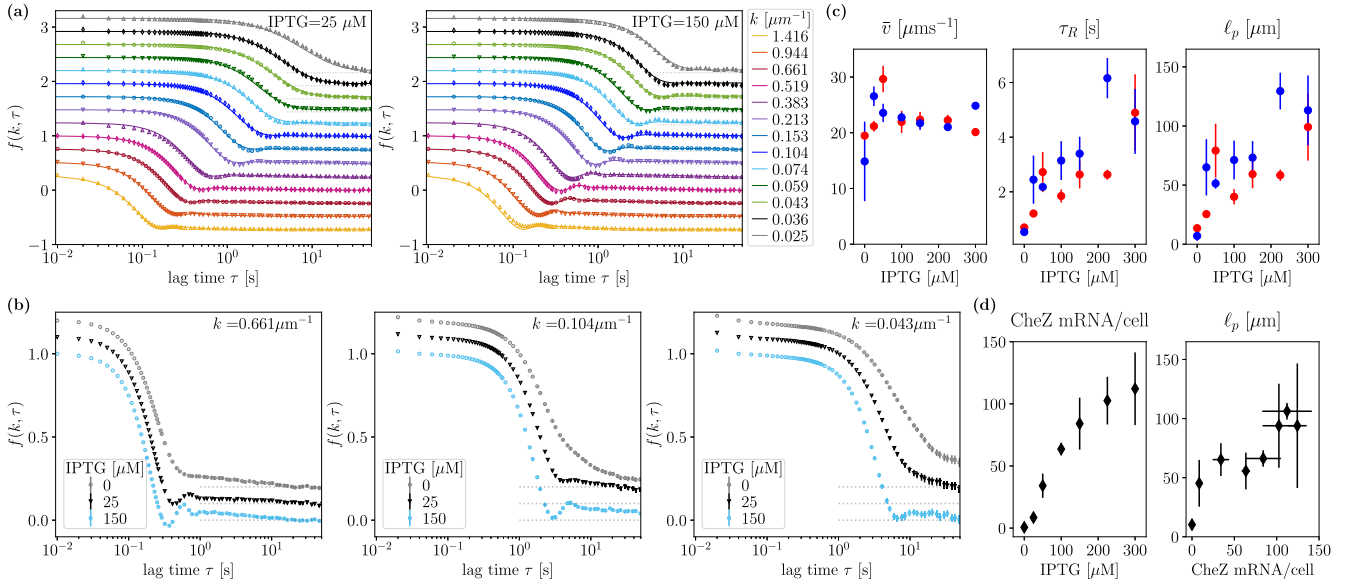

FIG. 3. Engineered *E. coli* strain NZ1. (a) ISFs for IPTG concentrations 25 and 150 μM. The ISFs are shifted vertically and gray dotted lines correspond to $f = 0$. Symbols and lines represent experiments and fits to the theory, respectively, and different colors correspond to different wave numbers k. (b) Comparison of the ISFs for different IPTG concentrations and wave numbers. (c) Average speed $\bar{v}$, run time τ_R, and persistence length ℓ_p, as a function of IPTG concentration. Red and blue symbols correspond to two biological replicates. The error is estimated from successive measurements of the ISF using the same sample. (d) Independent measurements of the number of CheZ mRNA per cell at various IPTG concentrations (left panel) allow correlating the persistence length ℓ_p and the number of CheZ mRNA per cell (right panel).

disentangling the contributions of diffusion, swimming, and tumbling to the dynamics (Fig. 2). Fitting Eq. (2) to data finally yields the set of kinetic parameters $\{\bar{v}, \sigma_v, \tau_R, \tau_T, \alpha, D\}$.

To measure the ISF experimentally, we imaged cells in sealed capillaries on a fully automated inverted bright-field microscope with a sCMOS camera. A full characterization of RT dynamics requires accessing length scales much greater than the persistence length ℓ_p in all directions. This necessitated a large depth of field at low k to ensure that bacteria remain in view over large distances in 3D. We thus consecutively recorded movies at 2× and 10× magnifications and extracted the corresponding ISFs for $k < 0.9\ \mu\text{m}^{-1}$ and $k \geq 0.9\ \mu\text{m}^{-1}$ using DDM [44,56], which are then fitted to our renewal theory using a numerical protocol described elsewhere [54].

IPTG-induced transition from tumbling to swimming.— We grew suspensions of the NZ1 strain at several IPTG concentrations and measured the ISFs. Representative data over approximately four decades in time and two decades in length are shown in Fig. 3(a). Oscillations typical of persistent swimmers (Fig. 2) are seen most clearly at the higher IPTG concentration and high k values.

In more detail, Fig. 3(b) compares the ISFs at a given k for three IPTG concentrations. In the absence of IPTG, diffusion dominates and the oscillations are absent. At IPTG = 25 μM, oscillations are seen for $k = 0.66\ \mu\text{m}^{-1}$ and $k = 0.1\ \mu\text{m}^{-1}$ (corresponding to length scales of $\sim 2\pi/k \approx 10$ and 60 μm, respectively), while data at the smallest k shows a smooth decay: the RT dynamics becomes effectively diffusive on such a large scale. At the highest IPTG concentration, 150 μM, oscillations are seen at all scales, showing a strong enhancement of the persistence length. To our knowledge, this is the first demonstration of a controlled tuning of the 3D gait of *E. coli* by varying external conditions.

Our protocol also allows us to quantify phenotypic heterogeneity. We repeated such measurements for eight IPTG concentrations, using two biological replicates and typically three to four successive measurements of $f(k, \tau)$ per replicate and IPTG concentration. The fitted kinetic parameters are then averaged for each replicate and plotted in Fig. 3(c). The small error bars show that successive measurements of $f(k, \tau)$ at each condition and for each biological replicate yielded consistent results. The observed variability between replicates (compare red and blue data points) therefore quantifies the degree of phenotypic heterogeneity in a clonal population [66].

Increasing IPTG leads to a robust increase of the persistence length, $\ell_p = \bar{v}\tau_R$, which translates into oscillations in the ISF [Figs. 3(a) and 3(b)]. Capturing quantitatively such fine-grained features requires very good statistics, a narrow speed distribution, and a low fraction of nonmotile cells, a challenge that is met by the experimental protocol described in [55]. Finally, note that there is little variability in the average speed ($\bar{v} \simeq 23.5\ \mu\text{m}^{-1}$ at all finite IPTG concentrations), the tenfold increase in ℓ_p

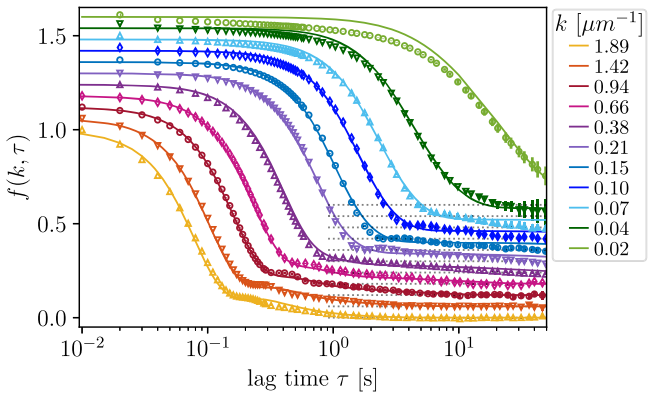

FIG. 4. Measurements of the ISFs for a WT *E. coli* suspension (symbols). Fits to Eq. (2) (lines) lead to $\bar{v} = 15.95\ \mu\mathrm{m\,s^{-1}}$, $\sigma_v = 5.78\ \mu\mathrm{m\,s^{-1}}$, $D = 0.24\ \mu\mathrm{m^2\,s^{-1}}$, $\alpha = 0.96$, $\tau_R = 2.39$ s, and $\tau_T = 0.38$ s. The ISFs are shifted vertically as in Fig. 3(a).

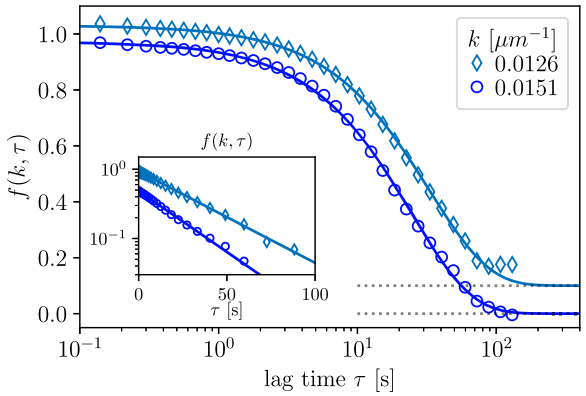

FIG. 5. Measured ISFs of WT *E. coli* at $k = 0.0126\ \mu\mathrm{m^{-1}}$ and $k = 0.0151\ \mu\mathrm{m^{-1}}$ (symbols) fitted against the ISF of diffusive particles (lines), giving effective diffusivities $D_{\mathrm{eff}} = 192\ \mu\mathrm{m^2\,s^{-1}}$ and $D_{\mathrm{eff}} = 178\ \mu\mathrm{m^2\,s^{-1}}$, respectively. The ISFs are shifted vertically as in Fig. 3(a).

results from longer run durations. This shows that the expression level of CheZ thus impacts tumbling statistics without altering the bacteria swimming speed.

Given the high speed of our NZ1 strain and the long run durations at high IPTG concentrations, the extraction of τ_R requires sampling large length scales, at which we find that the tumbling times τ_T cannot be reliably measured. We have tested the robustness of our results with respect to τ_T by fixing it at $\tau_T = 0.1, 0.2, 0.3$ s and extracting the remaining kinetic parameters. We find that the average velocity of the bacteria remains unaffected and the systematic increase of the persistence length persists (Fig. S1 [55]). Finally, while measurements of the evolution of single-motor statistics of wilde-type (WT) *E. coli* in different environments have been reported before [23], Fig. 3(d) shows for the first time the measured correlation between ℓ_p and the number of CheZ mRNA in the cell.

Wild-type E. coli.—Figure 4 shows the measured ISFs for a dilute suspension of WT *E. coli* over approximately four decades in time and two decades in length. The ISFs display an intermediate plateau at large k, which is a signature of the diffusive motion of both the small nonmotile fraction ($\lesssim 5\%$) and of the tumbling cells. The plateau disappears at low k and long times, which reflects the randomization of the swimming direction.

The WT data are well fitted by our renewal theory [54] at all k (Fig. 4, solid lines). We find that $96 \pm 0.1\%$ of the bacteria swim at a mean speed $\bar{v} = 16 \pm 0.1\ \mu\mathrm{m\,s^{-1}}$ with standard deviation $\sigma_v = 5.78 \pm 0.13\ \mu\mathrm{m\,s^{-1}}$ (errors are obtained by a jackknife resampling method [67]).

The lower WT speed (cf. $\bar{v} \approx 24\ \mu\mathrm{m\,s^{-1}}$ for NZ1) allows us to fit the mean run and tumble durations: $\tau_R = 2.39 \pm 0.11$ s (so that $\ell = \bar{v}\tau_R = 38 \pm 2\ \mu$m) and $\tau_T = 0.38 \pm 0.02$ s, giving a run fraction of $p_R = \tau_R/(\tau_R + \tau_T) \simeq 0.86$. Original, and still widely cited, measurements also gave $p_R \simeq 0.86$, but with $\tau_R = 0.86 \pm 0.20$ s and $\tau_T = 0.14 \pm 0.03$ s [1]. These results were obtained by tracking 35 bacteria, while we averaged over $\sim 10^4$–10^6 bacteria.

Finally, our data allow us to probe a range of length and time scales large enough to bridge short-scale directed swimming and large-scale diffusive motion. This is an important challenge since recent experiments have questioned the experimental relevance of exponentially distributed run and tumble durations [22,27]. The ISF of purely diffusive particles, $f(k,\tau) = A\exp(-k^2 D_{\mathrm{eff}}\tau)$, where A is a constant, gives a good account of our large-scale data (shown for two values of k in Fig. 5). Averaging over our two smallest values of k leads to $\langle D_{\mathrm{eff}}\rangle = 185 \pm 7\ \mu\mathrm{m^2\,s^{-1}}$.

In an RT model with exponentially distributed run and tumble durations, $\langle D_{\mathrm{eff}}^{\mathrm{th}}\rangle = (\bar{v}^2 + \sigma_v^2)\tau_R^2/(3\tau_R + 3\tau_T)$. Using parameters from fitting the measured ISF (caption, Fig. 4), we find $\langle D_{\mathrm{eff}}^{\mathrm{th}}\rangle = 198 \pm 11\ \mu\mathrm{m^2\,s^{-1}}$, which is remarkably close to the measured value. Interestingly, the σ_v^2 term arising from velocity fluctuations contributes to $\sim 10\%$ of the value of $\langle D_{\mathrm{eff}}^{\mathrm{th}}\rangle$. Note that our measured D_{eff} is 3 orders of magnitude larger than the fitted single-particle diffusivity, $D = 0.24 \pm 0.01\ \mu\mathrm{m^2\,s^{-1}}$, which highlights the ability of our protocol to provide information on active-particle dynamics over a large spatiotemporal range.

Conclusion.—By characterizing the dynamics of *E. coli* over a wide range of length and time scales, we demonstrated for the first time how the tumbling dynamics of an engineered strain can be tuned independently of the swimming speed. Furthermore, we have characterized to a high statistical accuracy the full 3D gait of WT *E. coli* in bulk suspensions, directly characterizing for the first time both the small-scale persistent motion and the large-scale diffusion. We have shown that a microscopic run and tumble model with exponentially distributed run and tumble durations describes both regimes. The use of more realistic distributions [27] can be accommodated in our approach, but is unlikely to change significantly any of our

conclusions. We also note that, while our bulk approach is well suited to characterize the population-scale distribution of motility gaits, cell tracking remains a very useful tool to investigate more precisely the detail of single-cell trajectories and investigate their diversity [1,27,63,68].

Our Letter lays the foundation for the high-throughput study of the swimming gait of a variety of microorganisms, such as the RT pattern of *Bacillus subtilis* [63] or the run-reverse motion of marine bacteria [69] and archaea [70], using standard microscopy. We hope that this will allow for a more systematic characterization of the role of cell motility in collective self-organization, which is often studied at a purely macroscopic scale due to the long-standing difficulty in characterizing cell motion at the microscopic level [71]. We note that the ability of microorganisms to respond to chemical fields or gradients, through quorum sensing or chemotaxis, is a vital part of their foraging and survival strategy. Our method, in combination with spatiotemporally resolved DDM [20], opens the way to the high-throughput study of such response at the population level.

This work was supported by the Austrian Science Fund (FWF) via P35580-N and the Erwin Schrödinger fellowship (J4321-N27), the European Research Council Grant No. AdG-340877-PHYSAPS, the ANR grant Bactterns, the Shenzhen Peacock Team Project (KQTD2015033117210153), and the National Key Research and Development Program of China (2021YFA0910700).

C. K. and Y. Z. contributed equally to this work.

*Corresponding author: ckurzthaler@pks.mpg.de
†Corresponding author: yfzhao2021@suda.edu.cn
‡Corresponding author: julien.tailleur@univ-paris-diderot.fr
§Corresponding author: vincent.martinez@ed.ac.uk

[1] H. C. Berg and D. A. Brown, Chemotaxis in *Escherichia coli* analysed by three-dimensional tracking, Nature (London) **239**, 500 (1972).
[2] H. C. Berg, *E. coli in Motion*, Biological and Medical Physics, Biomedical Engineering (Springer Science and Business Media, New York, 2008).
[3] J. Schwarz-Linek, J. Arlt, A. Jepson, A. Dawson, T. Vissers, D. Miroli, T. Pilizota, V. A. Martinez, and W. C. Poon, *Escherichia coli* as a model active colloid: A practical introduction, Colloids Surf. B **137**, 2 (2016).
[4] O. Pohl, M. Hintsche, Z. Alirezaeizanjani, M. Seyrich, C. Beta, and H. Stark, Inferring the chemotactic strategy of *P. putida* and *E. coli* using modified Kramers-Moyal coefficients, PLoS Comput. Biol. **13**, e1005329 (2017).
[5] I. H. Riedel, K. Kruse, and J. Howard, A self-organized vortex array of hydrodynamically entrained sperm cells, Science **309**, 300 (2005).
[6] B. M. Friedrich and F. Jülicher, The stochastic dance of circling sperm cells: Sperm chemotaxis in the plane, New J. Phys. **10**, 123025 (2008).
[7] S. S. Merchant *et al.*, The *Chlamydomonas* genome reveals the evolution of key animal and plant functions, Science **318**, 245 (2007).
[8] H. Machemer, Ciliary activity and the origin of metachrony in *Paramecium*: Effects of increased viscosity, J. Exp. Biol. **57**, 239 (1972).
[9] P. Romanczuk, M. Bär, W. Ebeling, B. Lindner, and L. Schimansky-Geier, Active Brownian particles, Eur. Phys. J. Special Topics **202**, 1 (2012).
[10] J. Elgeti, R. G. Winkler, and G. Gompper, Physics of microswimmers—single particle motion and collective behavior: A review, Rep. Prog. Phys. **78**, 056601 (2015).
[11] C. Bechinger, R. Di Leonardo, H. Löwen, C. Reichhardt, G. Volpe, and G. Volpe, Active particles in complex and crowded environments, Rev. Mod. Phys. **88**, 045006 (2016).
[12] J. O'Byrne, Y. Kafri, J. Tailleur, and F. van Wijland, Time irreversibility in active matter, from micro to macro, Nat. Rev. Phys. **4**, 167 (2022).
[13] O. Bénichou, C. Loverdo, M. Moreau, and R. Voituriez, Intermittent search strategies, Rev. Mod. Phys. **83**, 81 (2011).
[14] G. H. Wadhams and J. P. Armitage, Making sense of it all: Bacterial chemotaxis, Nat. Rev. Mol. Cell Biol. **5**, 1024 (2004).
[15] W. C. K. Poon, From *Clarkia* to *Escherichia* and Janus: The physics of natural and synthetic active colloids, in *Physics of Complex Colloids*, edited by C. Bechinger, F. Sciortino, and P. Ziherl (Società Italiana di Fisica, Bologna, 2013), pp. 317–386.
[16] X.-L. Wu and A. Libchaber, Particle diffusion in a quasi-two-dimensional bacterial bath, Phys. Rev. Lett. **84**, 3017 (2000).
[17] C. Liu, X. Fu, L. Liu, X. Ren, C. K. Chau, S. Li, L. Xiang, H. Zeng, G. Chen, L.-H. Tang *et al.*, Sequential establishment of stripe patterns in an expanding cell population, Science **334**, 238 (2011).
[18] A. Curatolo, N. Zhou, Y. Zhao, C. Liu, A. Daerr, J. Tailleur, and J. Huang, Cooperative pattern formation in multi-component bacterial systems through reciprocal motility regulation, Nat. Phys. **16**, 1152 (2020).
[19] C. Chen, S. Liu, X.-q. Shi, H. Chaté, and Y. Wu, Weak synchronization and large-scale collective oscillation in dense bacterial suspensions, Nature (London) **542**, 210 (2017).
[20] J. Arlt, V. A. Martinez, A. Dawson, T. Pilizota, and W. C. K. Poon, Dynamics-dependent density distribution in active suspensions, Nat. Commun. **10**, 2321 (2019).
[21] V. A. Martinez, E. Clément, J. Arlt, C. Douarche, A. Dawson, J. Schwarz-Linek, A. K. Creppy, V. Škultéty, A. N. Morozov, H. Auradou, and W. C. K. Poon, A combined rheometry and imaging study of viscosity reduction in bacterial suspensions, Proc. Natl. Acad. Sci. U.S.A. **117**, 2326 (2020).
[22] P. Cluzel, M. Surette, and S. Leibler, An ultrasensitive bacterial motor revealed by monitoring signaling proteins in single cells, Science **287**, 1652 (2000).

[23] E. Korobkova, T. Emonet, J. M. Vilar, T. S. Shimizu, and P. Cluzel, From molecular noise to behavioural variability in a single bacterium, Nature (London) **428**, 574 (2004).
[24] P. S. Lovely and F. Dahlquist, Statistical measures of bacterial motility and chemotaxis, J. Theor. Biol. **50**, 477 (1975).
[25] M. J. Schnitzer, Theory of continuum random walks and application to chemotaxis, Phys. Rev. E **48**, 2553 (1993).
[26] M. E. Cates and J. Tailleur, When are active Brownian particles and run-and-tumble particles equivalent? Consequences for motility-induced phase separation, Europhys. Lett. **101**, 20010 (2013).
[27] N. Figueroa-Morales, R. Soto, G. Junot, T. Darnige, C. Douarche, V. A. Martinez, A. Lindner, and E. Clément, 3D spatial exploration by *E. coli* echoes motor temporal variability, Phys. Rev. X **10**, 021004 (2020).
[28] P. Galajda, J. Keymer, P. Chaikin, and R. Austin, A wall of funnels concentrates swimming bacteria, J. Bacteriol. **189**, 8704 (2007).
[29] A. Sokolov, M. M. Apodaca, B. A. Grzybowski, and I. S. Aranson, Swimming bacteria power microscopic gears, Proc. Natl. Acad. Sci. U.S.A. **107**, 969 (2010).
[30] R. Di Leonardo, L. Angelani, D. Dell'Arciprete, G. Ruocco, V. Iebba, S. Schippa, M. P. Conte, F. Mecarini, F. De Angelis, and E. Di Fabrizio, Bacterial ratchet motors, Proc. Natl. Acad. Sci. U.S.A. **107**, 9541 (2010).
[31] H. H. Wensink, J. Dunkel, S. Heidenreich, K. Drescher, R. E. Goldstein, H. Löwen, and J. M. Yeomans, Meso-scale turbulence in living fluids, Proc. Natl. Acad. Sci. U.S.A. **109**, 14308 (2012).
[32] J. Saragosti, V. Calvez, N. Bournaveas, B. Perthame, A. Buguin, and P. Silberzan, Directional persistence of chemotactic bacteria in a traveling concentration wave, Proc. Natl. Acad. Sci. U.S.A. **108**, 16235 (2011).
[33] D. Nishiguchi, K. H. Nagai, H. Chaté, and M. Sano, Long-range nematic order and anomalous fluctuations in suspensions of swimming filamentous bacteria, Phys. Rev. E **95**, 020601(R) (2017).
[34] I. Grobas, M. Polin, and M. Asally, Swarming bacteria undergo localized dynamic phase transition to form stress-induced biofilms, eLife **10**, e62632 (2021).
[35] Z. Alirezaeizanjani, R. Großmann, V. Pfeifer, M. Hintsche, and C. Beta, Chemotaxis strategies of bacteria with multiple run modes, Sci. Adv. **6**, eaaz6153 (2020).
[36] G. Frangipane, D. Dell'Arciprete, S. Petracchini, C. Maggi, F. Saglimbeni, S. Bianchi, G. Vizsnyiczai, M. L. Bernardini, and R. Di Leonardo, Dynamic density shaping of photokinetic *E. coli*, eLife **7**, e36608 (2018).
[37] J. Arlt, V. A. Martinez, A. Dawson, T. Pilizota, and W. C. Poon, Painting with light-powered bacteria, Nat. Commun. **9**, 768 (2018).
[38] J. R. Howse, R. A. L. Jones, A. J. Ryan, T. Gough, R. Vafabakhsh, and R. Golestanian, Self-motile colloidal particles: From directed propulsion to random walk, Phys. Rev. Lett. **99**, 048102 (2007).
[39] A. Bricard, J.-B. Caussin, N. Desreumaux, O. Dauchot, and D. Bartolo, Emergence of macroscopic directed motion in populations of motile colloids, Nature (London) **503**, 95 (2013).
[40] J. Yan, M. Han, J. Zhang, C. Xu, E. Luijten, and S. Granick, Reconfiguring active particles by electrostatic imbalance, Nat. Mater. **15**, 1095 (2016).
[41] T. Bäuerle, A. Fischer, T. Speck, and C. Bechinger, Self-organization of active particles by quorum sensing rules, Nat. Commun. **9**, 3232 (2018).
[42] M. N. van der Linden, L. C. Alexander, D. G. A. L. Aarts, and O. Dauchot, Interrupted motility induced phase separation in aligning active colloids, Phys. Rev. Lett. **123**, 098001 (2019).
[43] D. Nishiguchi and M. Sano, Mesoscopic turbulence and local order in janus particles self-propelling under an ac electric field, Phys. Rev. E **92**, 052309 (2015).
[44] V. A. Martinez, R. Besseling, O. A. Croze, J. Tailleur, M. Reufer, J. Schwarz-Linek, L. G. Wilson, M. A. Bees, and W. C. K. Poon, Differential dynamic microscopy: A high-throughput method for characterizing the motility of micro-organisms, Biophys. J. **103**, 1637 (2012).
[45] H. C. Berg and L. Turner, Chemotaxis of bacteria in glass capillary arrays, *Escherichia coli*, motility, microchannel plate, and light scattering, Biophys. J. **58**, 919 (1990).
[46] W. R. DiLuzio, L. Turner, M. Mayer, P. Garstecki, D. B. Weibel, H. C. Berg, and G. M. Whitesides, *Escherichia coli* swim on the right-hand side, Nature (London) **435**, 1271 (2005).
[47] E. Lauga, W. R. DiLuzio, G. M. Whitesides, and H. A. Stone, Swimming in circles: Motion of bacteria near solid boundaries, Biophys. J. **90**, 400 (2006).
[48] R. Di Leonardo, D. Dell'Arciprete, L. Angelani, and V. Iebba, Swimming with an image, Phys. Rev. Lett. **106**, 038101 (2011).
[49] M. Molaei, M. Barry, R. Stocker, and J. Sheng, Failed escape: Solid surfaces prevent tumbling of *Escherichia coli*, Phys. Rev. Lett. **113**, 068103 (2014).
[50] B. Liu, M. Gulino, M. Morse, J. X. Tang, T. R. Powers, and K. S. Breuer, Helical motion of the cell body enhances *Caulobacter crescentus* motility, Proc. Natl. Acad. Sci. U.S.A. **111**, 11252 (2014).
[51] T. Darnige, N. Figueroa-Morales, P. Bohec, A. Lindner, and E. Clément, Lagrangian 3D tracking of fluorescent microscopic objects in motion, Rev. Sci. Instrum. **88**, 055106 (2017).
[52] J. Sheng, E. Malkiel, and J. Katz, Digital holographic microscope for measuring three-dimensional particle distributions and motions, Appl. Opt. **45**, 3893 (2006).
[53] S. Bianchi, F. Saglimbeni, and R. Di Leonardo, Holographic imaging reveals the mechanism of wall entrapment in swimming bacteria, Phys. Rev. X **7**, 011010 (2017).
[54] Y. Zhao, C. Kurzthaler, N. Zhou, J. Schwarz-Linek, C. Devailly *et al.*, companion paper, Quantitative characterization of run-and-tumble statistics in bulk bacterial suspensions, Phys. Rev. E **109**, 014612 (2023).
[55] See Supplemental Material at http://link.aps.org/supplemental/10.1103/PhysRevLett.132.038302, which includes Refs. [3,17,44,54,56–59], for details on the experiments and the fitting procedure.
[56] L. G. Wilson, V. A. Martinez, J. Schwarz-Linek, J. Tailleur, G. Bryant, P. N. Pusey, and W. C. K. Poon, Differential dynamic microscopy of bacterial motility, Phys. Rev. Lett. **106**, 018101 (2011).

[57] M. Reufer, V. A. Martinez, P. Schurtenberger, and W. C. K. Poon, Differential dynamic microscopy for anisotropic colloidal dynamics, Langmuir **28**, 4618 (2012).
[58] R. Cerbino and V. Trappe, Differential dynamic microscopy: Probing wave vector dependent dynamics with a microscope, Phys. Rev. Lett. **100**, 188102 (2008).
[59] C. Kurzthaler, C. Devailly, J. Arlt, T. Franosch, W. C. K. Poon, V. A. Martinez, and A. T. Brown, Probing the spatiotemporal dynamics of catalytic Janus particles with single-particle tracking and differential dynamic microscopy, Phys. Rev. Lett. **121**, 078001 (2018).
[60] A. Celani and M. Vergassola, Bacterial strategies for chemotaxis response, Proc. Natl. Acad. Sci. U.S.A. **107**, 1391 (2010).
[61] S. Chatterjee, R. A. da Silveira, and Y. Kafri, Chemotaxis when bacteria remember: Drift versus diffusion, PLoS Comput. Biol. **7**, e1002283 (2011).
[62] L. Angelani, Averaged run-and-tumble walks, Europhys. Lett. **102**, 20004 (2013).
[63] L. Turner, L. Ping, M. Neubauer, and H. C. Berg, Visualizing flagella while tracking bacteria, Biophys. J. **111**, 630 (2016).
[64] Since bacteria are anisotropic, a single D is a crude surrogate of the short-time diffusivity matrix elements, but it helps to fit experimental data of swimming cells. A full matrix description requires a larger fraction of passive cells and a different model [65], and is outside our scope.
[65] C. Kurzthaler, S. Leitmann, and T. Franosch, Intermediate scattering function of an anisotropic active Brownian particle, Sci. Rep. **6**, 36702 (2016).
[66] M. B. Elowitz, A. J. Levine, E. D. Siggia, and P. S. Swain, Stochastic gene expression in a single cell, Science **297**, 1183 (2002).
[67] B. Efron, Nonparametric estimates of standard error: The jackknife, the bootstrap and other methods, Biometrika **68**, 589 (1981).
[68] G. Junot, T. Darnige, A. Lindner, V. A. Martinez, J. Arlt, A. Dawson, W. C. K. Poon, H. Auradou, and E. Clément, Run-to-tumble variability controls the surface residence times of E. coli bacteria, Phys. Rev. Lett. **128**, 248101 (2022).
[69] J. E. Johansen, J. Pinhassi, N. Blackburn, U. L. Zweifel, and Å. Hagström, Variability in motility characteristics among marine bacteria, Aquat. Microb. Ecol. **28**, 229 (2002).
[70] K. L. Thornton, J. K. Butler, S. J. Davis, B. K. Baxter, and L. G. Wilson, Haloarchaea swim slowly for optimal chemotactic efficiency in low nutrient environments, Nat. Commun. **11**, 4453 (2020).
[71] J. D. Murray, *Mathematical Biology: I. An Introduction* (Springer, New York, 2002).